

---

01 Jan 1980

## Large-angle Electron-photon Coincidence Experiment In Atomic Hydrogen

E. Weigold

L. Frost

K. (Kaare) J. Nygaard

*Missouri University of Science and Technology*

Follow this and additional works at: [https://scholarsmine.mst.edu/phys\\_facwork](https://scholarsmine.mst.edu/phys_facwork)

 Part of the [Physics Commons](#)

---

### Recommended Citation

E. Weigold et al., "Large-angle Electron-photon Coincidence Experiment In Atomic Hydrogen," *Physical Review A*, vol. 21, no. 6, pp. 1950 - 1954, American Physical Society, Jan 1980.

The definitive version is available at <https://doi.org/10.1103/PhysRevA.21.1950>

This Article - Journal is brought to you for free and open access by Scholars' Mine. It has been accepted for inclusion in Physics Faculty Research & Creative Works by an authorized administrator of Scholars' Mine. This work is protected by U. S. Copyright Law. Unauthorized use including reproduction for redistribution requires the permission of the copyright holder. For more information, please contact [scholarsmine@mst.edu](mailto:scholarsmine@mst.edu).

## Large-angle electron-photon coincidence experiment in atomic hydrogen

E. Weigold, L. Frost, and K. J. Nygaard\*

*Institute of Atomic Studies, School of Physical Sciences, The Flinders University of South Australia, Bedford Park, South Australia*

(Received 5 July 1979)

1s-2p excitation in hydrogen has been studied by observing the angular correlation of Lyman  $\alpha$  photons detected in coincidence with inelastically scattered electrons at 54.4 eV incident energy. The electron scattering angles ranged from  $10^\circ$  to  $133^\circ$ ; the results at scattering angles larger than  $20^\circ$  cannot be explained by currently available theories.

We have recently studied electron-photon coincidences in atomic hydrogen<sup>1,2</sup> at small electron scattering angles ( $\theta_e = 10\text{--}20^\circ$ ) at incident energies of 40, 54.4, 70, 100, and 200 eV. The salient feature of this communication is that we have now extended the electron scattering angle to  $133^\circ$  for 54.4-eV incident electrons and still obtained a satisfactory coincidence signal-to-noise ratio. Electron excitation of atomic hydrogen presents the simplest inelastic collision process. Nevertheless, theoretical amplitudes for excitation of the 2p level of hydrogen exhibit significant differences for  $\theta_e \geq 20^\circ$ , as will be discussed later. The major objective of this work has, therefore, been to obtain reliable electron-photon angular correlations which can be used to test the validity of the theories at large momentum transfer.

Specifically, we have studied the process



in which the excited hydrogen atoms (lifetime 1.6 nsec) decay by emission of Lyman  $\alpha$  photons (121.6 nm), by detecting the uv photons in coincidence with inelastically scattered electrons that have suffered a characteristic energy loss of 10.2 eV.

For  $s \rightarrow p$  transitions in hydrogen, the electron-photon coincidence count rate is given by<sup>3</sup>

$$\frac{d^4 N_e(k_i^2)}{d\Omega_e d\Omega_\gamma dz dt} = \frac{3}{8\pi} \frac{I_e}{e} \rho(z) \epsilon_e \epsilon_\gamma \sigma_p K, \quad (2)$$

where  $\rho(z)$  is the target atom number density at point  $z$ ,  $I_e/e$  is the number of incident electrons passing through the interaction region per second,  $\epsilon_e$  and  $\epsilon_\gamma$  are, respectively, the overall efficiencies for detecting inelastically scattered electrons and photons, and  $d\Omega_e$  and  $d\Omega_\gamma$  are the respective differential solid angles. Furthermore, the angular correlation  $K$  is described by

$$K(k_i^2, \Omega_e, \Omega_\gamma) = \frac{1}{18} [11 + 3\lambda + (1 - 3\lambda) \cos^2 \theta_\gamma + 6\sqrt{2} R \sin(2\theta_\gamma) \cos(\phi_e - \phi_\gamma) - 3(1 - \lambda) \sin^2 \phi_\gamma \cos 2(\phi_e - \phi_\gamma)], \quad (3)$$

which in our coplanar geometry ( $\phi_e - \phi_\gamma = \pi$ ) reduces to

$$9K = [3\lambda + 4 + 3(1 - 2\lambda) \cos^2 \theta_\gamma - 3\sqrt{2} R \sin 2\theta_\gamma]. \quad (4)$$

From the experimental angular correlations, we can therefore determine the important parameters

$$\lambda \equiv \sigma_0 / \sigma_p \quad (5)$$

and

$$R \equiv \text{Re} \langle a_0 a_1 \rangle / \sigma_p, \quad (6)$$

where  $\sigma_0 = \langle a_0 a_0 \rangle$  is the differential cross section for excitation of the  $m_l = 0$  substate, and  $\sigma_1 = \langle a_1 a_1 \rangle$  for the  $m_l = \pm 1$  substates,  $a_0$  and  $a_1$  being the corresponding amplitudes, and we define  $\sigma_p \equiv \sigma_0 + 2\sigma_1$ .

The general layout of the apparatus and the techniques used are discussed in detail by Hood *et al.*<sup>2,4</sup> In brief, hydrogen atoms were produced in a direct-current electrical discharge<sup>4</sup> and allowed to effuse through a small aperture into the interaction region with an atom number density of about  $10^{18} \text{ m}^{-3}$ . The divergence of the electron beam was less than  $0.5^\circ$  and the opening angle of the electron analyzer less than  $2^\circ$ . The major improvement over the previous apparatus is that we used chevron-mounted multichannel plates to detect the Lyman  $\alpha$  photons instead of a channel electron multiplier. The circular multichannel plate detector subtended a full opening angle of  $15^\circ$  at the interaction region. Such an opening angle does not significantly distort the angular correlations in the case of atomic hydrogen, where the angular correlation is relatively isotropic, being confined to the range  $4 \leq 9K \leq 7$  (Eq. 4).

The electron-photon coincidence count rate was corrected for background pulses in the usual way.<sup>2</sup> With the channel plates and improved electronics, the timing resolution was less than 3 nsec FWHM. Owing to low net count rates at large electron scattering angles, typical data accumulation times at a fixed angle were as high as 14 days in order to obtain adequate statistical accuracy.

Problems arising from long-term drifts in

TABLE I. The experimental angular correlations normalized to the expression  $9K$  (Eq. 4). The figures in brackets give the one-standard-deviation statistical errors.

$\theta_e = 25^\circ$		$\theta_e = 30^\circ$		$\theta_e = 40^\circ$		$\theta_e = 50^\circ$		$\theta_e = 60^\circ$		$\theta_e = 80^\circ$		$\theta_e = 100^\circ$		$\theta_e = 133^\circ$	
$\theta_\gamma$	$9K$	$\theta_\gamma$	$9K$	$\theta_\gamma$	$9K$	$\theta_\gamma$	$9K$	$\theta_\gamma$	$9K$	$\theta_\gamma$	$9K$	$\theta_\gamma$	$9K$	$\theta_\gamma$	$9K$
139	6.20 (0.23)	139	5.85 (0.28)	139	6.44 (0.42)	139	6.38 (0.40)	139	5.79 (0.45)	139	5.90 (0.81)	139	7.14 (1.29)	139	2.63 (1.85)
130	6.31 (0.23)	130	6.65 (0.29)	135	5.77 (1.11)	130	6.87 (0.41)	130	6.26 (0.46)	130	5.33 (0.83)	130	5.97 (1.30)	130	5.72 (1.94)
120	6.36 (0.24)	120	5.69 (0.28)	130	6.05 (0.36)	120	6.61 (0.41)	120	6.83 (0.47)	120	5.12 (0.84)	120	5.87 (1.31)	120	7.88 (2.00)
110	5.94 (0.23)	110	6.06 (0.29)	120	6.28 (0.36)	110	6.38 (0.41)	110	6.12 (0.47)	110	4.30 (0.84)	110	5.52 (1.30)	110	10.3 (2.1)
100	5.16 (0.23)	100	5.45 (0.28)	110	7.05 (0.37)	100	7.36 (0.41)	100	7.30 (0.55)	100	6.72 (0.86)	100	5.89 (1.30)	100	6.10 (2.01)
90	5.35 (0.23)	90	6.02 (0.28)	100	6.02 (0.45)	90	7.06 (0.40)	90	7.42 (0.47)	90	6.69 (0.85)	90	5.06 (1.27)	90	10.9 (2.07)
80	4.92 (0.23)	80	5.47 (0.27)	90	6.70 (0.36)	70	6.74 (0.39)	80	6.47 (0.54)	80	8.31 (0.85)	80	4.60 (1.26)	80	4.99 (1.95)
70	4.75 (0.23)	70	4.87 (0.27)	80	5.46 (0.43)	60	5.93 (0.39)	70	7.30 (0.46)	70	5.62 (0.83)	70	6.81 (1.27)	70	5.57 (1.95)
60	4.57 (0.22)	60	4.90 (0.27)	70	5.93 (0.35)	50	4.92 (0.38)	60	5.44 (0.53)	60	6.59 (0.83)	60	5.84 (1.25)	60	6.57 (1.93)
50	4.83 (0.23)	50	4.49 (0.26)	60	4.64 (0.51)	40	4.13 (0.38)	50	5.70 (0.46)	50	5.00 (0.82)	50	4.28 (1.24)	50	5.99 (1.91)
40	4.66 (0.23)	40	5.05 (0.27)	50	5.05 (0.41)	30	4.71 (0.39)	40	5.07 (0.45)	40	5.54 (0.83)	40	6.03 (1.27)	40	5.64 (1.92)
30	4.99 (0.24)	30	5.10 (0.32)	40	5.49 (0.41)	20	3.57 (0.39)	30	4.71 (0.46)	30	5.92 (0.85)	30	5.98 (1.29)	30	6.01 (1.96)
20	5.13 (0.24)	20	5.07 (0.28)	30	4.36 (0.40)	10	3.56 (0.43)	20	4.11 (0.47)	20	4.50 (0.88)	20	6.92 (1.35)	20	5.07 (2.02)
		15	5.21 (0.29)	25	3.68 (1.47)			10	2.89 (0.52)	10	3.52 (1.01)	10	3.77 (1.66)	10	4.67 (2.72)
		20	4.75 (0.39)	20	4.75 (0.39)			-15	4.94 (1.73)			-20	8.94 (1.51)	-20	3.58 (2.15)
		15	4.63 (0.66)	15	4.63 (0.66)			-30	6.32 (1.05)			-30	2.74 (1.34)	-30	6.27 (2.11)
		10	3.43 (0.55)	10	3.43 (0.55)			-35	5.36 (0.89)			-40	4.78 (1.30)	-40	5.40 (1.99)
												-50	3.85 (1.28)	-50	5.10 (1.95)
												-55	3.48 (1.26)	-60	4.06 (1.89)
												-70	2.23 (1.87)	-70	2.23 (1.87)
												-80	5.81 (1.86)	-80	5.81 (1.86)
												-85	6.68 (1.88)	-85	6.68 (1.88)

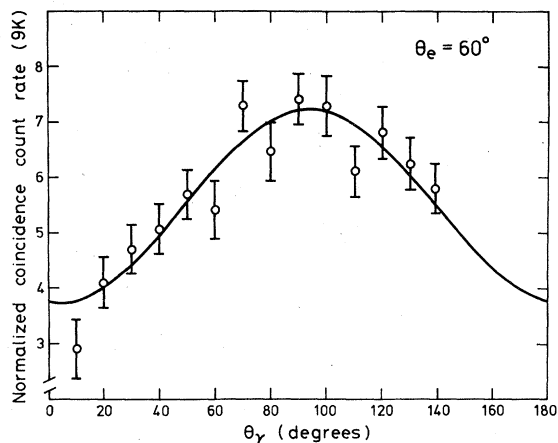


FIG. 1. Normalized coincidence count rate plotted against the photon detection angle at an electron scattering angle of  $60^\circ$  and incident electron energy of 54.4 eV. The full curve is the best fit to  $9K$  (Eq. 4) yielding values of  $\lambda = 1.07 \pm 0.08$  and  $R = 0.07 \pm 0.04$ .

either hydrogen beam density or electron current were overcome by scanning repeatedly over the whole angular range  $\theta_\gamma$ , and as a further check during each scan, each measurement at a given  $\theta_\gamma$  was repeated four times nonsequentially. The range of  $\theta_\gamma$  during each run was usually from  $(\theta_e$

+  $45^\circ$ ) to  $139^\circ$ , where for convenience the angles  $\theta_e$  are denoted by negative values.

Since the pulses from the photon detectors start the time-to-amplitude converter<sup>2</sup> (TAC), care must be taken to ensure that the variation in dead time of the TAC at the different photon angles due to the different photon count rates does not influence the data. With the present photon count rates ( $<10^4$  Hz) and the observed variation in count rates as a function of angle ( $<1.5 \times 10^3$  Hz) and TAC dead time ( $5 \mu\text{sec}$ ), this correction is always less than 0.5%.

Table I lists the experimental angular correlations normalized to the expression  $9K$ . In Fig. 1, we display the normalized coincidence count rate versus photon detection angle  $\theta_\gamma$  at the constant electron scattering angle  $\theta_e = 60^\circ$ . The full curve is the result of fitting the angular coincidence count rate to the function  $9K$  (Eq. 4) using a  $\chi^2$  technique previously discussed.<sup>2</sup> For the specific example shown, best agreement is obtained with  $\lambda = 1.07 \pm 0.08$  and  $R = 0.07 \pm 0.04$ . Although the values of  $R$  and  $\lambda$  are interdependent and their mutual accuracy is most properly described as an error locus,<sup>2</sup> for ease of comparison with the theory we present them separately as displayed in Figs. 2 and 3, respectively. The data at  $\theta_e = 10^\circ$ ,

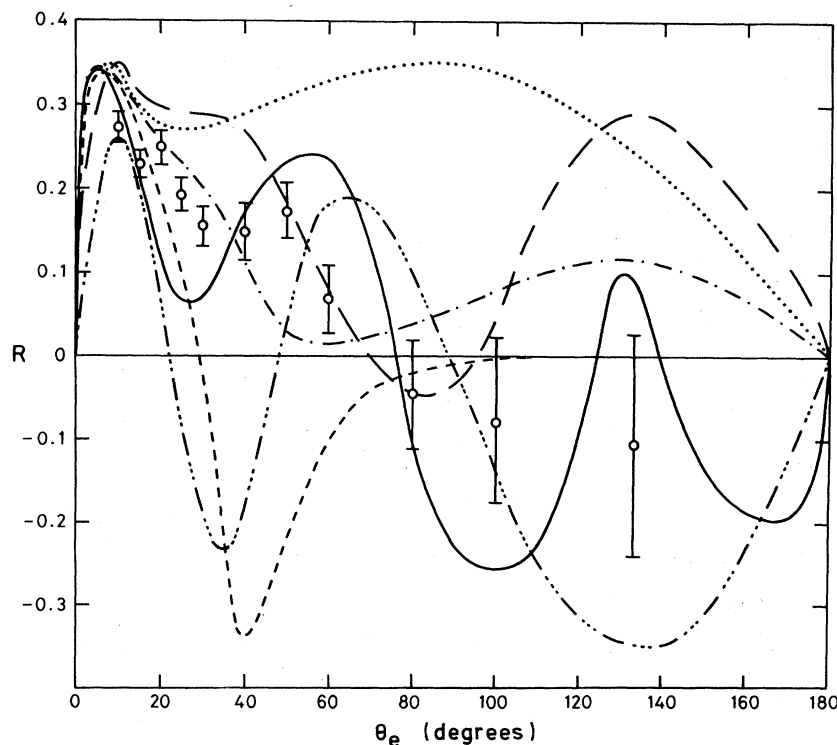


FIG. 2. The parameter  $R$  [Eq. (6)] as a function of electron scattering angle  $\theta_e$  at an incident energy of 54.4 eV. The experimental points are shown as open circles with associated error bars:  $\dots$  Born approximation;  $---$  DWPO<sup>5</sup>;  $- \cdot -$  DWBA<sup>6</sup>;  $----$  UGA<sup>7</sup>;  $----$  CPTM<sup>8</sup>; and  $—$  hybrid CC.<sup>9</sup>

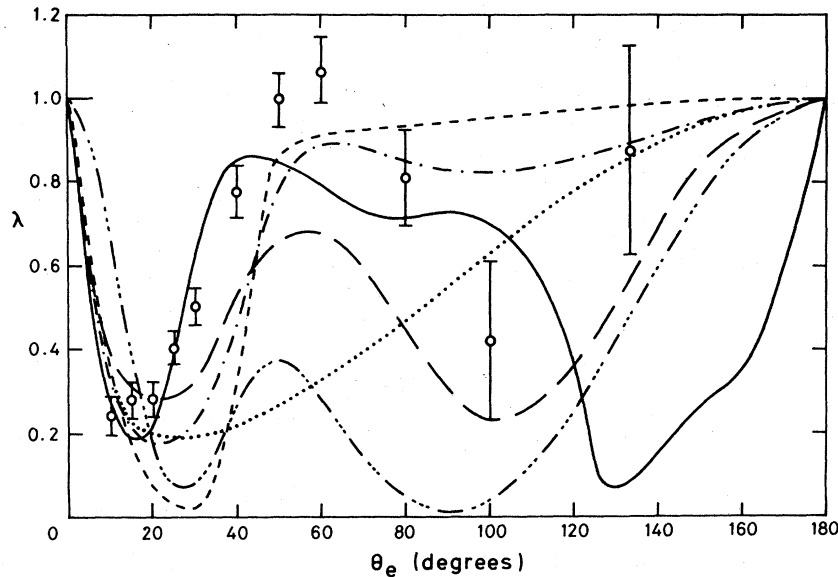


FIG. 3. The parameter  $\lambda$  [Eq. (5)] as a function of  $\theta_e$  at an incident energy of 54.4 eV. The theoretical curves are identified in Fig. 2.

TABLE II. Values of the parameters  $\lambda$  and  $\text{Re} \langle a_0 a_1 \rangle / \sigma$  obtained from various calculations and the  $\chi^2$  probabilities of the resulting fits to the experimental data at the various electron scattering angles and magnitudes of the momentum transfer. The direction of the momentum transfer can be obtained from the Born approximation value of  $\lambda$  using  $\lambda_B = \cos^2 \theta_B$ . DWPO—Morgan and McDowell 1975; DWBA—Calhoun *et al.* 1977; UGA—Gau and Macek 1975; CPTM—Roberts 1977; MCC—Callaway *et al.* 1976.

$\theta_e$ [ $K(a_0^{-1})$ ]	$\lambda$ $\text{Re} \langle a_0 a_1 \rangle / \sigma$ $P(\chi^2)$						
	Best fit	Born	DWPO <sup>a</sup>	DWBA	UGA <sup>a</sup>	CPTM	MCC
	0.404 (39)	0.188	0.29	0.19	0.035	0.079	0.391
25°	0.194 (20)	0.276	0.29	0.228	0.10	-0.07	0.068
[0.84]	0.80	0	0.0001	0	0	0	0
	0.503 (42)	0.192	0.33	0.212	0.02	0.076	0.628
30°	0.155 (24)	0.278	0.29	0.201	-0.02	-0.18	0.073
[1.00]	0.20	0	0	0	0	0	0.001
	0.778 (62)	0.222	0.53	0.454	0.35	0.263	0.856
40°	0.149 (34)	0.294	0.27	0.115	-0.334	-0.18	0.174
[1.31]	0.23	0	0.0001	0	0	0	0.12
	0.995 (64)	0.27	0.66	0.781	0.86	0.376	0.843
50°	0.174 (34)	0.314	0.18	0.031	-0.22	0.04	0.234
[1.62]	0.21	0	0	0	0	0	0.02
	1.07 (8)	0.33	0.675	0.89	0.91	0.285	0.794
60°	0.068 (41)	0.333	0.0008	0.014	-0.10	0.18	0.238
[1.91]	0.35	0	0	0.03	0	0	0
	0.81 (12)	0.474	0.45	0.856	0.93	0.048	0.715
80°	-0.045 (64)	0.353	-0.043	0.039	-0.03	0.10	-0.102
[2.45]	0.19	0	0.01	0.13	0.15	0	0.13
	0.41 (17)	0.629	0.23	0.825	0.95	0.04	0.701
100°	-0.065 (90)	0.342	0.05	0.079	0.0	-0.13	-0.255
[2.92]	0.20	0.0008	0.11	0.03	0.02	0.05	0.04
	0.87 (25)	0.86	0.57 <sup>b</sup>	0.89 <sup>b</sup>	0.98 <sup>b</sup>	0.48 <sup>b</sup>	0.08 <sup>b</sup>
133°	-0.11 (13)	0.245	0.29 <sup>b</sup>	0.12 <sup>b</sup>	0.0 <sup>b</sup>	-0.35 <sup>b</sup>	0.09 <sup>b</sup>
[3.45]	0.49	0.18	0.088	0.34	0.45	0.14	0.03

<sup>a</sup> Calculated at 50 eV and parameters estimated from published graphs.

<sup>b</sup> Parameters taken from Figs. 2 and 3.

15°, and 20° are those of Hood *et al.*<sup>2</sup>

The calculated values of  $R$  and  $\lambda$  were obtained using the Born, distorted-wave polarized orbital<sup>5</sup> (DWPO), distorted-wave Born<sup>6</sup> (DWBA), unrestricted Glauber<sup>7</sup> (UGA), classical-path  $T$ -matrix<sup>8</sup> (CPTM), and hybrid close-coupling<sup>9</sup> (CC) approximations. We point out that the DWPO and UGA calculations were done for an incident energy of 50 eV.

In Table II we give the best-fit values of  $\lambda$  and  $R$  with corresponding probabilities. Also included in Table II are the  $\chi^2$  probabilities obtained using the various theoretical values of  $\lambda$  and  $R$ , with the normalization varied to minimize  $\chi^2$ . Perusal of Table II, and Figs. 2 and 3 shows that the agreement between experiment and theory, and between the various theories is almost nonexistent for scattering angles above 20°. In the angular range 20°–40° the hybrid close-coupling calculation gives good values of  $\lambda$  but significantly underestimates  $R$ . At larger angles, the curves show that there may be convergence problems in the calculation. This is to be expected at 54.4 eV and large momentum transfer since the close-coupling method was used only for partial waves with  $l \leq 3$  in the partial-wave expansion of the total wave function. The unitarized Born approximation was used for higher partial waves. An improved calculation is in progress.<sup>10</sup>

In the same angular region the DWBA gives reasonable values of  $R$  but significantly underestimates  $\lambda$ . The DWPO method, which also involves the decomposition of the total wave function into partial waves, predicts a trend for  $\lambda$  which is similar to that observed but yields quite poor values of  $R$  in certain angular regions. Although the UGA and CPTM calculations both give the explicit Rutherford behavior at large momentum transfer, they differ significantly in their predictions for  $\lambda$  and  $R$ , and both are in serious disagreement with experiment.

The failure of the UGA at all but the smallest angles is not surprising since at larger angles it

considerably underestimates the  $1s - (2s + 2p)$  differential cross sections measured by Williams and Willis.<sup>11</sup> The CPTM approximation is a simple impulse approximation which does not include the effects of exchange. It is therefore more likely to be accurate at higher energies and large scattering angles.

The DWPO calculation allows for polarization of the target in the incident channel, and the incident channel continuum wave corresponds to an adiabatic-exchange function. At angles smaller than 50°, it is in good agreement with the  $1s - (2s + 2p)$  experimental differential cross sections, but at larger angles it considerably underestimates them. The problem could, however, be in the  $1s - 2s$  cross section calculation. The DWBA includes exchange but no polarization effects. The potential in both incident and exit channels is taken as the interaction with the static  $H(1s)$  potential. It gives  $1s - (2s + 2p)$  differential cross sections in quite good agreement with the experimental values. The hybrid close-coupling distorted-wave model of Callaway *et al.*<sup>9</sup> gives  $1s - (2s + 2p)$  cross sections in excellent agreement with the data. It is the most detailed of the calculations. The disagreement with the present data is probably due to the convergence problems discussed above.

The variation of the  $\lambda$  parameter with the angle is quantitatively very similar to that obtained for the  $1s - 2p \ ^1P$  transition in He at 81.2 eV by Hollywood *et al.*<sup>12</sup> They found that none of the published theoretical values agreed with their data over the entire angular range. We similarly find, for the simplest and most fundamental inelastic collision process, that although the published theoretical values of  $\lambda$  and  $R$  differ markedly, none are able to reproduce the experimental values over the whole measured angular range.

We gratefully acknowledge support of this work by the Australian Research Grants Committee, the Department of Science (Australia), and the National Science Foundation (USA).

\*Permanent address: Department of Physics, University of Missouri-Rolla, Rolla, Mo. 65401.

<sup>1</sup>A. J. Dixon, S. T. Hood, and E. Weigold, *Phys. Rev. Lett.* **40**, 1262 (1978).

<sup>2</sup>S. T. Hood, E. Weigold, and A. J. Dixon, *J. Phys. B* **12**, 631 (1979).

<sup>3</sup>J. H. Macek and D. H. Jaecks, *Phys. Rev. A* **4**, 2288 (1971).

<sup>4</sup>S. T. Hood, A. J. Dixon, and E. Weigold, *J. Phys. E* **11**, 948 (1978).

<sup>5</sup>L. A. Morgan and M. R. C. McDowell, *J. Phys. B* **8**, 1073 (1975).

<sup>6</sup>R. V. Calhoun, D. H. Madison, and W. N. Shelton, *J.*

*Phys. B* **10**, 3523 (1977).

<sup>7</sup>J. N. Gau and J. H. Macek, *Phys. Rev. A* **12**, 1760 (1975).

<sup>8</sup>M. J. Roberts, *J. Phys. B* **10**, 2219 (1977).

<sup>9</sup>J. Callaway, M. R. C. McDowell, and L. A. Morgan, *J. Phys. B* **9**, 2043 (1976).

<sup>10</sup>M. R. C. McDowell and L. A. Morgan (private communication).

<sup>11</sup>J. F. Williams and B. A. Willis, *J. Phys. B* **8**, 1641 (1975).

<sup>12</sup>M. T. Hollywood, A. Crowe, and J. F. Williams, *J. Phys. B* **12**, 819 (1979).